Control of a Wind Driven DFIG Connected to the Grid Based on Field Orientation

A.A. Hassan, Yehia S. Mohamed, A.M. El-Sawy, Mahmoud A. Mossa
Department of Electrical Engineering, Faculty of engineering, El-Minia Univeristy, Minia, Egypt
E_mail: eng_mahmoud2015@yahoo.com

ABSTRACT

Field orientation, with autonomous control of reactive power, using PI controller is the most widely used controlling method of doubly-fed induction generators (DFIG). This paper describes a method for separate control of active and reactive power of grid-connected DFIG using PI controller. Using MATLAB/SIMULINK software, the behavior of controller is evaluated during variation of wind speed. Simulation results represent the behavior of controller when facing the variations. This paper first explains the model of DFIG and the second part is explaining field oriented control of DFIG.

Keywords: DFIG, reactive power control of induction machines, PI controller.

LIST OF SYMBOLS

V_{ds}^{e}, V_{qs}^{e}	d^e-axis and q^e-axis stator voltages.
i_{ds}^{e}, i_{qs}^{e}	d^e-axis and q^e-axis stator currents.
V_{dr}^{e}, V_{qr}^{e}	d^e-axis and q^e-axis rotor voltages.
i_{dr}^{e}, V_{qr}^{e}	d^e-axis and q^e-axis rotor currents.
i_{md}^{e}, i_{mq}^{e}	d^e-axis and q^e-axis magnetizing currents.
V_{ds}^{s}, V_{qs}^{s}	d^s-axis and q^s-axis stator voltages.
i_{ds}^{s}, i_{as}^{s}	d^s-axis and q^s-axis stator currents.
i_{dr}^{s}, i_{qr}^{s}	d^s-axis and q^s-axis rotor currents.
R_S	stator winding resistance, Ω.
R_r	rotor winding resistance, Ω.
L_m	magnetizing inductance, H.
L_S	stator self inductance, H.
L_r	rotor self inductance, H.
L_{ls}	stator leakage inductance, H.
L_{lr}	rotor leakage inductance, H.
ω_r	electrical rotor angular speed in rad./sec.
V_W	wind speed, m./sec.
p	d/dt, the differential operator.
T_m	mechanical torque in the shaft, N.m.
T_e	electromagnetic torque, N.m.
B	friction damping coefficient, N.m./rad./sec.
J_m	machine moment of inertia, Kg.m^2.
P_S, Q_S	stator active and reactive power.
P_m	turbine power, W.

P	number of pole pairs.
θ_e	electrical stator flux angle.
θ_r	electrical rotor flux angle.
θ_{slip}	electrical slip flux angle.
β	blade pitch angle, degree.
μ	ratio of the rotor blade tip speed and wind speed.
ρ	specific density of the air, Kg.m^3.
$C_p(\beta, \mu)$	turbine power coefficient.
D_r	rotor diameter in meters.

Subscripts

d-q	direct and quadrature axis.
s,r	stator and rotor, respectively.
*	denote the reference value.
^	denote the estimated value.

1. INTRODUCTION

Wind electrical power system are recently getting lot of attention, because they are cost competitive, environmental clean and safe renewable power sources, as compared fossil fuel and nuclear power generation. A special type of induction generator, called a doubly fed induction generator (DFIG), is used extensively for high-power wind applications. They are used more and more in wind turbine applications due to easy controllability, high energy efficiency and improved power quality.

Fixed speed generators and induction generators had the disadvantage of having low power efficiencies at most speeds. Turbines are commonly installed in rural areas with unbalanced power transmission grids [7] and [9]. For an induction machine an unbalanced grid imposes negative effects like overheating and mechanical stress due to torque pulsations.

For example for an unbalance of 6% the induction generator is stopped from generating to the grid. By control of the rotor currents of a DFIG, the effects of unbalanced stator voltages may be compensated for. DFIG's ability to control rotor currents allows for reactive power control and variable speed operation, so it can operate at maximum efficiency over a wide range of wind speeds [2] and [4]. The doubly-Fed Induction Generator (DFIG) is widely used for variable-speed generation and it is one of the most important generators for wind energy conversion systems (WECS).

Variable-speed power plants using DFIG_s and field orientation method, in this method, the maximum use of wind energy powers us to control reactive power [11]. In DFIG control methods, rotor current regulation controls the power produced by stator. This leads to a huge reduction in size and cost of converter.

In this paper a method for control of reactive power of grid- connected DFIG using PI controller is adopted. Using MATLAB/SIMULINK software, the behavior of controller is evaluated during variation of wind speed. Simulation results represent the behavior of controller when facing the variations. This paper first explains the model of DFIG and the second part is explaining field oriented control of DFIG.

2. SYSTEM DESCRIPTION

Figure 1. shows a basic layout of a DFIG wind turbine system, the machine may be simulated as an induction machine having 3-phase supply in the stator and three phase supply in the

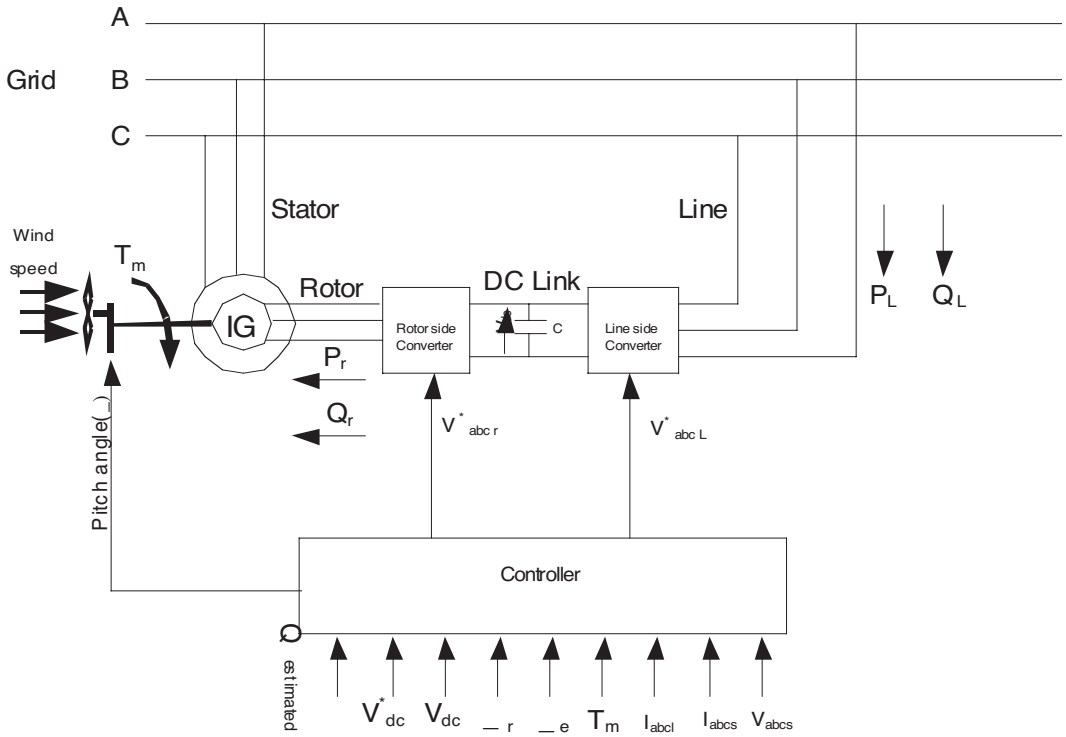

Figure 1: Wind turbine and doubly-fed induction generator system.

rotor. The rotor circuit is connected through slip rings to the back to back converters arrangement controlled by pulse width modulation (PWM) strategies [10] and [11]. The rated of these converters are restricted for speed range operation to a fraction of the machine rated power.

The voltage magnitude and power direction between the rotor and the supply may be varied by controlling the switch impulses that drive the IGBTs inverter. Back to back converters consist of two voltage source converters (ac-dc-ac) having a dc link capacitor connecting them. The generator side converter takes the variable frequency voltage and converts it into a dc voltage. The grid side converter has the ac voltage from the dc link as input and voltage at grid as output.

Rotor-side converter acts as a voltage source converter, while the grid-side convertor is expected to keep the capacitor voltage under wind speed changes and at different operating conditions of the grid [12] and [13].

3. DYNAMIC MODELING OF THE DFIG

3.1. Turbine model

In wind parks, many wind turbines are equipped with fixed frequency induction generators. Thus the power generated is not optimized for all wind conditions. To operate a wind turbine at its optimum at different wind speeds, the wind turbine should be operated at its maximum power coefficient ($C_{p(\beta,\mu),\text{optimum}} = 0.3\text{-}0.5$).

To operate around its maximum power coefficient, the wind turbine should be operated at a constant tip-speed ratio, which is proportional to ratio of the rotor speed to the wind speed. As the wind speed increases, the rotor speed should follow the variation of the wind speed [19]. In general, the load to the wind turbine is regulated as a cube function of the rotor rpm to

operate the wind turbine at the optimum efficiency. The aerodynamic power generated by wind turbine can be written as:

$$P_m = 0.5\rho A V_w^3 C_p(\beta,\mu) \tag{1}$$

Where ρ is the specific density of the air, the swept area of the blades (A) and the wind speed (V_w), $C_p(\beta, \mu)$ is the power conversion function, which is commonly defined in terms of the ratio of the rotor blade tip speed (μ) and the wind speed (V_w) as following:

$$C_p(\beta,\mu) = 0.73\left(\frac{151}{\mu} - 0.002\beta - 13.2\right)e^{\frac{18.4}{\mu}} \tag{2}$$

Where

$$\mu = \frac{D_r \omega_r}{2V_w} \tag{3}$$

The power coefficient function in (2), is shown in Fig. 2 parameterized in function of the pitch angle.

At lower wind speed, the pitch angle is set to a null value, because, the maximum power coefficient is obtained for this angle. Pitch angle control operates only when the value for wind speed is greater than the nominal wind speed [14].

To operate the wind turbine at its optimum efficiency $(C_{p(\beta,\mu),\text{optimum}})$ the rotor speed must be varied in the same proportion as the wind-speed variation. If we can track the wind speed precisely, the power can also be expressed in terms of the rotor speed.

In reality, the wind turbine rotor has a significantly large inertia due to the blade inertia and other components. The wind turbine operation can only in the vicinity. However, compared to fixed-speed operation, the energy captured in variable-speed operation is significantly higher.

Figure 3. shows the wind turbine control system, inputs to block are turbine speed (ω_r), pitch angle and wind speed (V_w), the turbine speed is obtained from the power-speed characteristics curve (tracking characteristics) of figure 4. The output from the block is the mechanical torque on the shaft

$$T_m = \frac{P_m}{\omega_r} \tag{4}$$

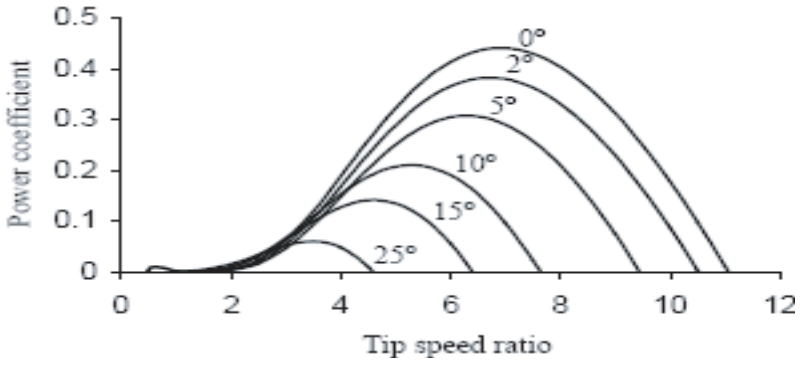

Figure2: Power coefficient $C_p(\beta, \mu)$ at different tip speed ratios .

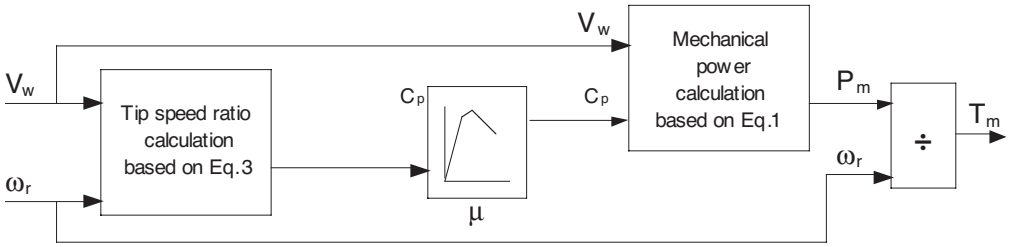

Figure 3: Wind turbine control system.

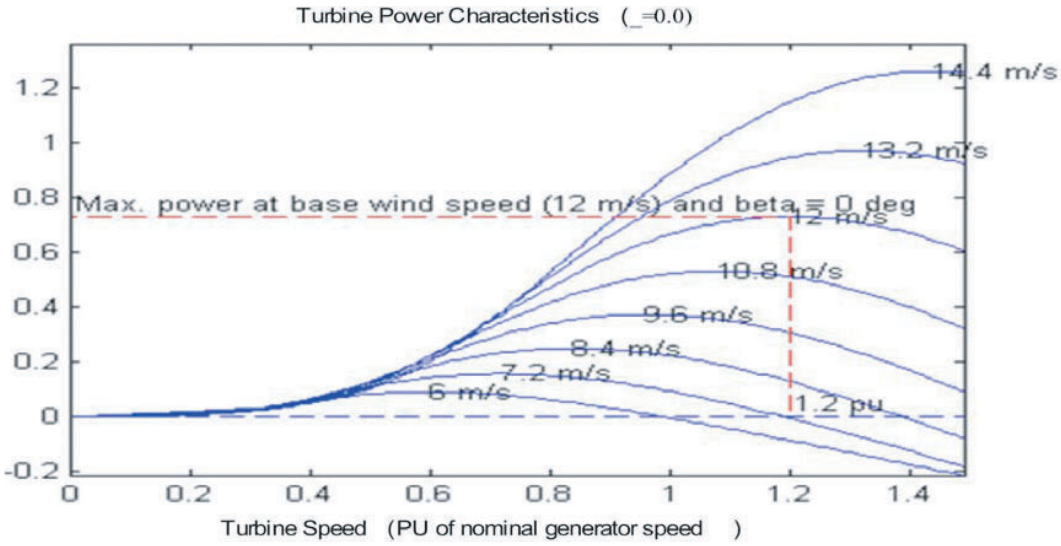

Figure 4: Power-speed characteristic curves of the wind turbine at different wind speeds and constant β.

3.2. Induction machine model

The induction machine can be modeled and represented in d^S - q^S reference frame as shown in figure 5.This representation is a general model based on the assumption that the supply voltage can be applied to both the stator and/or rotor terminals. The conventional model and the d^S - q^S axes model are the same for steady state analysis. The advantage of the d^S - q^S axes model is that it is powerful for analyzing the transient and steady state conditions, giving the complete solution of any dynamics [5] and [8]. The general equations for the d^S - q^S representation of an induction machine, in the stationary stator reference frame, are given as:

$$\begin{bmatrix} V_{ds}^s \\ V_{qs}^s \\ V_{dr}^s \\ V_{qr}^s \end{bmatrix} = \begin{bmatrix} R_s + pL_s & 0 & pL_m & 0 \\ 0 & R_s + pL_s & 0 & pL_m \\ pL_m & \omega_r L_m & R_r + pL_r & \omega_r L_r \\ -\omega_r L_m & pL_m & -\omega_r L_r & R_r + pL_r \end{bmatrix} \begin{bmatrix} i_{ds}^s \\ i_{qs}^s \\ i_{dr}^s \\ i_{qr}^s \end{bmatrix} \tag{5}$$

The developed electromagnetic torque can be expressed in terms of stator and rotor current components as:

$$T_e = \frac{3}{2}\frac{P}{2} L_m (i_{qs}^s i_{dr}^s - i_{ds}^s i_{qr}^s) \tag{6}$$

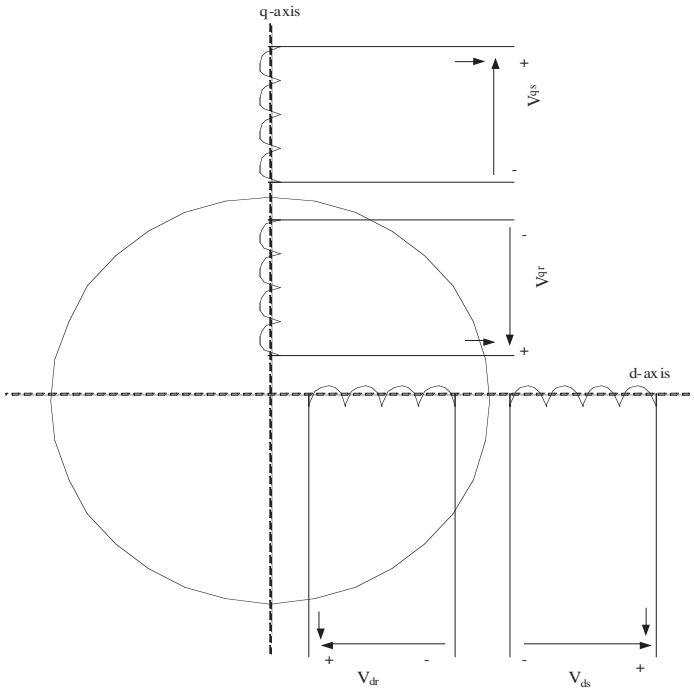

Figure 5: d-q axis representation of an induction machine.

The mechanical equation in the generating region is

$$T_m = J_m \frac{d\omega_\tau}{dt} + B\omega_r + T_e \tag{7}$$

The state-space form of equation (7) can be written as:

$$\frac{d\omega_r}{dt} = \frac{T_m - T_e - B\omega_r}{J_m}$$

These four first order differential equations in (5) are solved with the well known fourth order Runge-Kutta method to obtain the d^s- and q^s- axis leakage fluxes. These fluxes are related to the machine voltages and currents by the following equations

$$\lambda^s_{ds} = \int (V^s_{ds} - i^s_{ds} R_s)\ dt$$
$$\lambda^s_{qs} = \int (V^s_{qs} - i^s_{qs} R_s)\ dt \tag{8}$$
$$\theta_e = \tan^{-1} \frac{\lambda^s_{qs}}{\lambda^s_{ds}}$$

$$\therefore \theta_{slip} = \theta_e - \theta_r \tag{9}$$

3.3. Effect of stator resistance variation and its compensation

The stator resistance changes due to change in temperature during the operation of the machine as the machine losses change. The variation of the stator resistance is a thermal process and therefore is not only determined by the machine losses but also by the time. The control system becomes unstable if controller instrumented stator resistance is higher than its actual value in the generator [17].

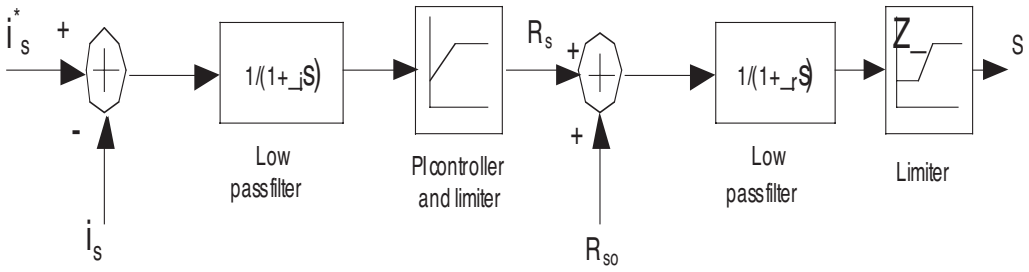

Figure 6: Block diagram schematic of the adaptive stator resistance compensator.

This may be reasoned as follows. As the generator resistance decreases, then its current increases for the same applied mechanical power, this increases the flux and electromagnetic torque. They are compared with their command (reference) values giving larger torque and flux linkages errors resulting in commanding larger voltages and hence in larger currents leading to a run off condition. The parameter mismatch between the controller and the machine also results in a nonlinear characteristic between torque and its reference making it a nonideal torque amplifier.

The generator resistance adaptation is essential to overcome instability and to guarantee a linear torque amplifier [19].

A block diagram schematic of the applied stator resistance compensation scheme is shown in Fig. 6. This technique is based on the principle that the error between the measured stator feedback current phasor i_S and its command i^*_S [12] is proportional to the stator resistance variation which is mainly caused by the generator temperature and to a smaller extent by the varying stator frequency.

The incremental value of stator resistance for correction is obtained through a PI controller and limiter. The current error goes through a low pass filter, which has very low cutoff frequency in order to remove high frequency components contained in the stator feedback current. This incremental stator resistance, ΔR_S

Is continuously added to the previously estimated stator resistance, R_{SO}. The final estimated value, R_S is obtained as the output of another low pass filter and limiter. This low pass filter is necessary for a smooth variation of the estimated resistance value. This final signal is the updated stator resistance and can be used directly in the controller. The stator feedback current phasor magnitude i_S is obtained from the q and d axis measured currents as,

$$i_s = \sqrt{\left(i_{ds}\right)^2 + \left(i_{qs}\right)^2} \tag{10}$$

The stator command (reference) current phasor magnitude i^*_S is derived from the dynamic equations of the induction motor in the synchronously rotating reference frame.

$$i_s^* = \sqrt{\left(i_{ds}^{e*}\right)^2 + \left(i_{qs}^{e*}\right)^2} \tag{11}$$

Where

$$i_{qs}^{e*} = \frac{2}{3}\frac{2}{P}\frac{T_e^*}{\lambda_{ds}^{e*}} \tag{12}$$

and i_{ds}^{e*} can be determined by solving the following equation

$$L_s\left(i_{ds}^{e*}\right)^2 - \lambda_{ds}^{e*}\left(1 - \frac{L_s L_r}{L_m^2 - L_s L_r}\right) i_{ds}^{e*} + L_s\left(i_{ds}^{e*}\right)^2 - \frac{\left(\lambda_{ds}^{e*}\right)^2 L_r}{L_m^2 - L_s L_r} = 0.0 \tag{13}$$

Equation (13) gives two solutions for i_{ds}^{e*} and the appropriate solution is the one that gives a smaller value.

Note that *d–q* axis stator current commands are independent of stator and rotor resistances and so is the stator current phasor command. In the implementation, these values are calculated and stored for various operating conditions.

3.4. Converter model

Mathematical modeling of converter system is realized by using various types of models, which can be broadly divided into two groups: mathematical functional models and Mathematical physical models (either equation-oriented or graphic-oriented, where graphic-oriented approach is actually based on the same differential equations).

In fact, it is assumed that the converters are ideal and the DC-link voltage between them is constant. Consequently, depending on the converter control, a controllable voltage (current) source can be implemented to represent the operation of the rotor-side of the converter in the model. Physical model as shown in figure 7, on the other hand [13] and [16], models constituting elements of the system separately and also considers interrelationship among different elements within the system, where type and structure of the model is normally dictated by the particular requirements of the analysis, e.g. steady-state. Indeed, due to the importance of more realistic production of the behavior of DFIG, it is intended to adopt physical model rather than functional model in order to accurately assess performance of DFIG in the event of fault particularly in determining whether or not the generator will trip following a fault.

This paper proposes a graphic-oriented switch-by-switch representation of the back-to-back PWM converters with their modulators for both rotor- and stator-side converters, where both IGBT and reverse diode devices are represented as a two-state resistive switch. The two-state switch can take on two values, R_{ON} (close to zero) and R_{OFF} (very high).

3.5. DC link model

The dc link capacitor provides dc voltage to the machine side converter and any attempt to store active power in the capacitor would raise its voltage level [9]. Thus to ensure stability of

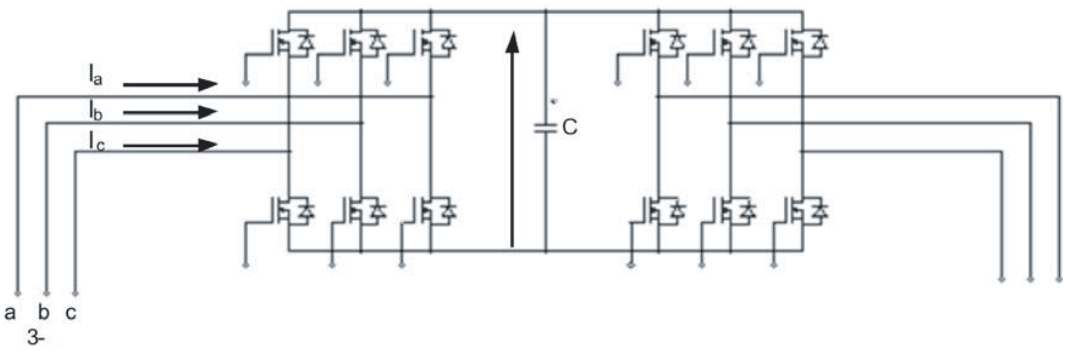

Figure 7: Physical model of converter system.

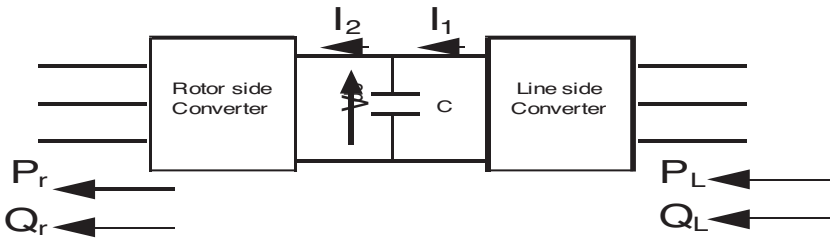

Figure 8: Power flow through dc-link element.

the system, power flow of the line side converter, as indicated in figure 8, should guarantee the following control objective:

$$P_1 = P_r \tag{14}$$

The dc link dynamic equation can be written as

$$C\frac{dv_{dc}}{dt} = i_1 - i_2 \tag{15}$$

In which V_{dc} is the dc bus voltage and C is the capacitance. Assuming no power losses for the converters, i_1 and i_2 can be derived as

$$i_1 = \frac{P_1}{V_{dc}} \tag{16}$$

$$i_2 = \frac{P_r}{V_{dc}} \tag{17}$$

Then from Eq. 15 through 17, as long as Eq. 14 is satisfied, the dc link voltage maintains stable, though small ripples might be present due to the instantaneous inequality between P_1 and P_r, and a small variation may occur during transient as a result of energy transferring.

4. FIELD ORIENTED CONTROL OF DFIG

The field orientation techniques allow decoupled or independent control of both active and reactive power. These techniques are based on the concept of $d^e - q^e$ controlling in different reference frames [14] and [15], where the current and the voltage are decomposed into distinct components related to the active and reactive power. In this work, the stator flux oriented rotor current control, with decoupled control of active and reactive power is adopted.

The control schemes for the doubly-fed induction machine are expected to track a prescribed maximum power curve, for maximum power capturing and to be able to control the reactive power generation. These control objectives must be achieved with adequate stability of the system which also includes the power converter and the dc link. The total active and reactive power generated can be calculated in terms of $d^e - q^e$ stator voltage and current components as [13]

$$P_s = \frac{3}{2}|V_s|i_{qs}^e \tag{18}$$

$$Q_s = \frac{3}{2}|V_s|i_{ds}^e \tag{19}$$

Where

$$|V_s| = \sqrt{(V_{ds}^e)^2 + (V_{qs}^e)^2}$$

The field orientation control is based on the field d^e - q^e model, where the reference frame rotates synchronously with respect to the stator flux linkage, with the d-axis of the reference frame instantaneously overlaps the axis of the stator flux. By aligning the stator flux phasor λ_s on the d^e - axis, so ($\omega = \omega_e$ and $\lambda_{qs} = 0$, $\lambda\varepsilon_{ds} = \lambda_s$). In such case the following expressions are obtained

$$\lambda_{qs}^e = L_s i_{qs}^e + L_m i_{qr}^e = 0$$

$$\therefore i_{qs}^e = -\frac{L_m}{L_s} i_{qr}^e \tag{20}$$

The developed electromagnetic torque can be expressed in terms of d^e - q^e stator current and flux components as:

$$T_e = \frac{3}{2}\frac{P}{2}(i_{qs}^e \lambda_{ds}^{\varepsilon} - i_{ds}^e \lambda_{qs}^{\varepsilon}) \tag{21}$$

By putting $\lambda_{qs}^{\varepsilon} = 0,$ in the above equation

$$\therefore T_e = \frac{3}{2}\frac{P}{2}(i_{qs}^e \lambda_{ds}^e) \tag{22}$$

Using (20) and the active power equation (18), the equation of the active power can be expressed as follows:

$$P_s = -\frac{3}{2}|V_s|\frac{L_m}{L_s} i_{qr}^e \tag{23}$$

The d^e-axis stator current component can be written as

$$= \frac{|V_s|}{2\pi f_s L_m} - i_{dr}^e \tag{24}$$

Using (22) and the reactive power equation (19), the equation of the reactive power can be expressed as follows:

$$Q_s = \frac{3}{2}|V_s|\left(\frac{|V_s|}{2\pi f_s L_m} - i_{dr}^{\varepsilon}\right) \tag{25}$$

Therefore, the d^e-axis rotor current component, $[i_{dr}^e]$ can be obtained to regulate the stator reactive power while the $q\varepsilon$-axis rotor current component, $[i_{qr}^e]$ can be obtained to regulate the stator active power and the generator speed [15] and [16]. As a result, the control of the stator active power $[P_s]$ via $[i_{qr}^e]$ as shown in Fig. 9 and the control of the stator reactive power $[Q_s]$ via $[i_{dr}^e]$ as shown in Fig. 10 are essentially decoupled, and so a separate decoupler is not necessary to implement field orientation control for the slip power recovery. Flux control is generally unnecessary, (since it would maintain a constant level, restricted by the constant magnitude and frequency of the line voltage), while the control of reactive power becomes possible.

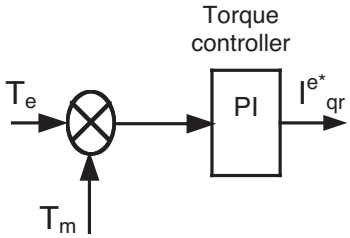

Figure.9: Torque controller

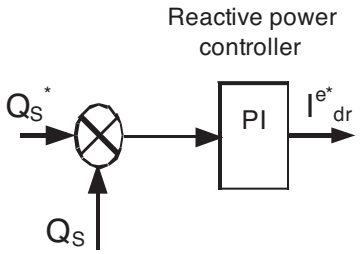

Figure.10: Reactive power controller

5. COMPLETE SYSTEM CONFIGURATION

Figure 11 shows the block diagram of controlling method. The control system consists of reactive power controller, torque controller, three current controllers, two co-ordinate transformation (C.T), and two current-regulated pulse-width-modulation (CRPWM) voltage source converters. Using 2-axis and 3-axis transforms, and transferring to the new reference frame, d and q components of machine parameters will be obtained. Having compared with reference values, the components return to their own reference frame and as a three-phase voltage will be used for switching the rotor-part converter [8] and [17]. The reference value of reactive power, Q_{sref}, can be either directly implemented to be convertor, considering the appropriate power, calculated from equations (23 and 25).

Individual control of the machine side converter and of the line side converter and related feedback between the two converters are shown. For speed control purpose, a PID type speed loop generates the torque command; for position control purpose, another loop with position errors precedes the speed loop. A current-regulated pulse-width-modulation (CRPWM) voltage source converter provides field oriented currents i_{dr} and i_{qr} to the rotor circuit, controlling stator reactive power and electromagnetic torque, respectively. The co-ordinate transformation (C.T) in Fig. 11 is used for transforming these components to the three phase rotor voltage commands by using the field angle.

Torque command is given by the turbine optimal torque-speed profile. Another (CRPWM) voltage source converter is used to interface with the power network, possibly through a transformer. In the same d-q reference frame as determined by the stator flux, its currents (I_{ql} and I_{dl}) are also field oriented, controlling P_L and Q_L, respectively. As discussed earlier, P_L is controlled through I_{ql} to stabilize the dc bus voltage and Q_L is controlled through I_{dl} to meet the overall reactive power command.

The method uses stator reference frame model of the induction machine and the same reference frame is used in the implementation thereby avoiding the trigonometric operations encountered in the C.T of other reference frames. This is one of the advantages of the control scheme.

6. RESULTS AND DISCUSSIONS

Digital simulation is carried out in order to validate the effectiveness of the proposed scheme of Fig. 7. The Matlab/Simulink software package has been used for this purpose. The DFIG under study is a 9 MW, 6-poles, 967 rpm, its nominal parameters and specifications are listed in table 1.

Results are taken while wind speed has increased from (8 to 14 m/sec). P_{sref} is implemented to turbine with respect to the optimum speed of turbine [19]. As can be seen in figure 6.3, during the transient state after each change in wind speed, the reactive power is kept constant.

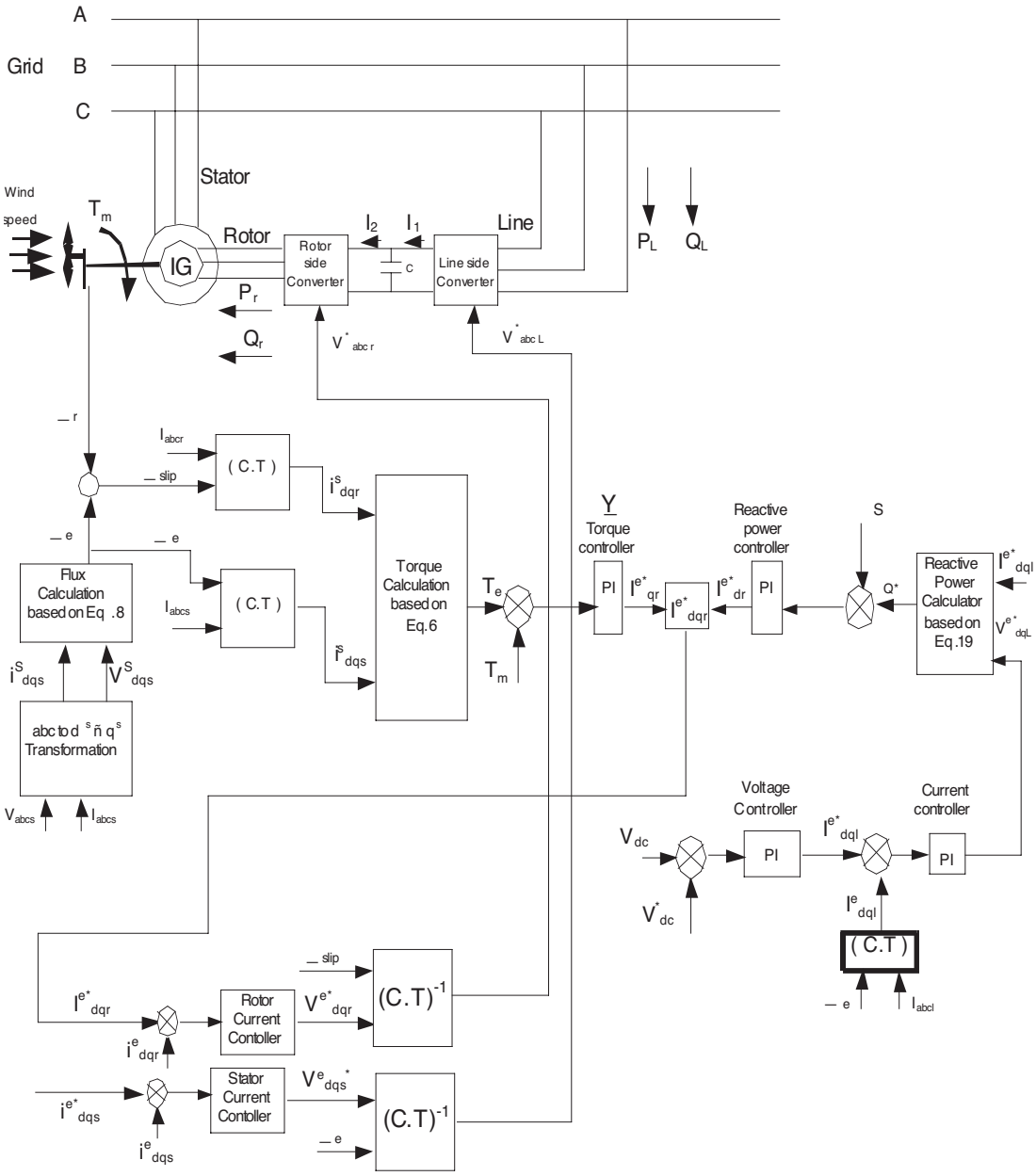

Figure 11: Proposed control scheme of the DFIG based on field orientation

Wind speed changes do not affect the value of reactive power produced by generator, and active power follows the power-speed curve of turbine .this clarifies the ability of controlling to separately the active and reactive power of stator.

It is noted from above results that at (t = 5 sec), the generated active power starts increasing smoothly (together with the turbine speed) to reach its rated value of 9 MW in approximately 20 sec. Over that time the turbine speed will have increased from 0.8 PU to 1.21 PU. Initially, the pitch angle of the turbine blades is zero degree and the turbine operating point follows the tracking characteristic curve of the turbine power up to maximum point.

Then the pitch angle is increased from 0 deg to 0.76 deg in order to limit the mechanical power. The reactive power is controlled to maintain a 1 PU voltage. At nominal power, the wind turbine absorbs 0.68 Mvar (generated Q = −0.68 Mvar) to control voltage at 1PU.

Table 1: The features of generator, wind turbine and controller

PI Controller	DFIG & Wind Turbine
Reactive Power Regulator	P_n(nominal) = 9*10^6 W.
Gains[kp,ki]=[0.05,5]	V_n(rms)= 580 V.
Active Power Regulator	F_n= 50 Hz.
Gains[kp,ki]=[1,100]	R_s= 0.104 Ω, L_{ls}= 2.54 (H)
DC Bus Regulator	R_r= 0.0743 Ω, L_{lr}= 2.31 (H)
Gains[kp,ki]=[0.002,0.05]	L_m= 4.35 (H)
Grid-side Converter	V_{dc}(nominal)= 1200 V.
Current Regulator	J_m = 0.0887 Kg.m^2
Gains[kp,ki]=[1,100]	B = 0.00478 N.m./rad./s.
Rotor-side Converter	DC bus capacitor = 6*10000e-6 F.
Current Regulator	Nominal mechanical output power of turbine = 9*10^6 W.
Gains[kp,ki]=[0.3,8]	At V_w = 12 m/s. ρ = 1.25 Kg./m^2.

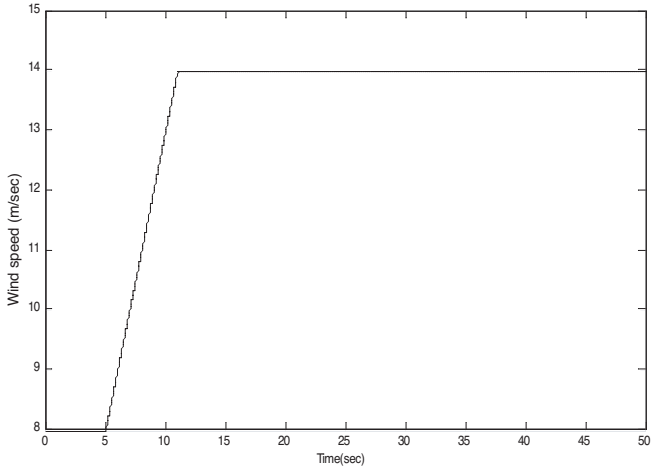

Figure 6.1: Wind speed (m/sec)

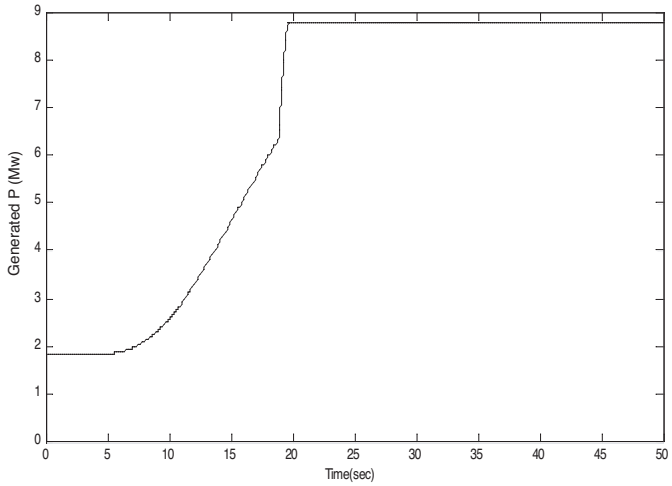

Figure 6.2: Generated active power

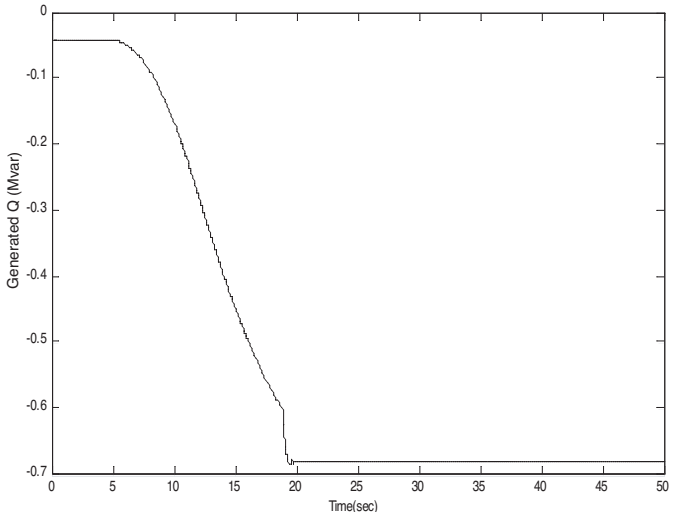

Figure 6.3: Generated reactive power

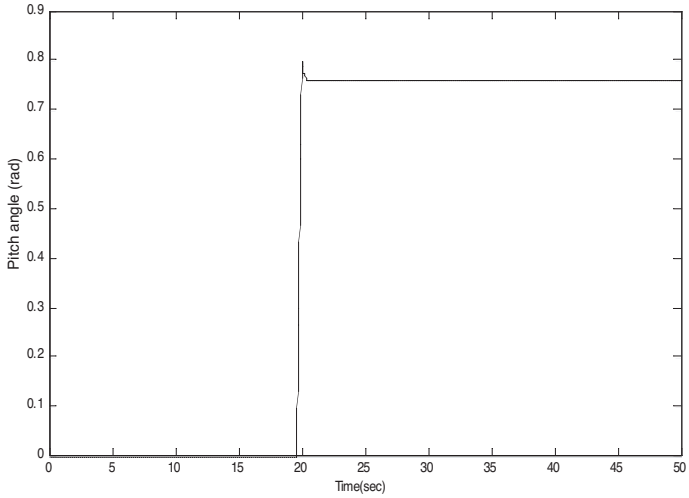

Figure 6.4: Pitch angle variation

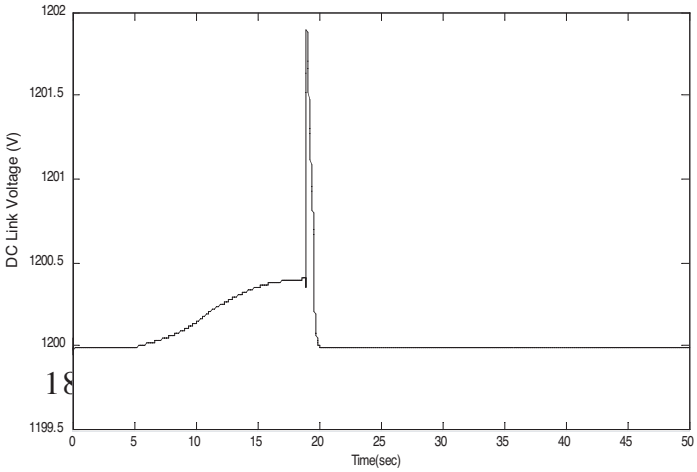

Figure 6.5: DC link voltage (volts)

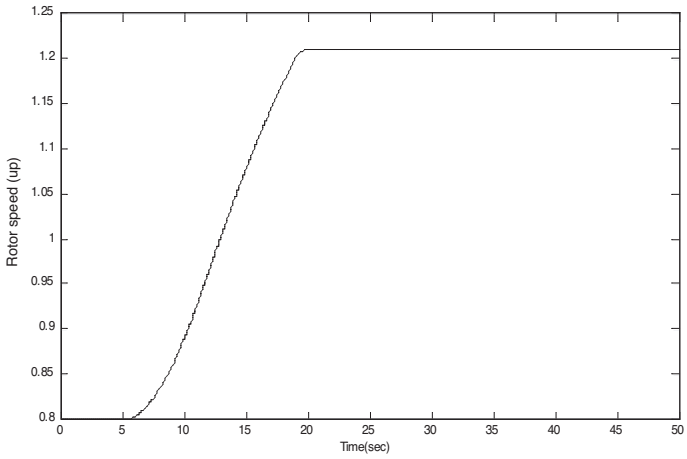

Figure 6.6: Rotor speed

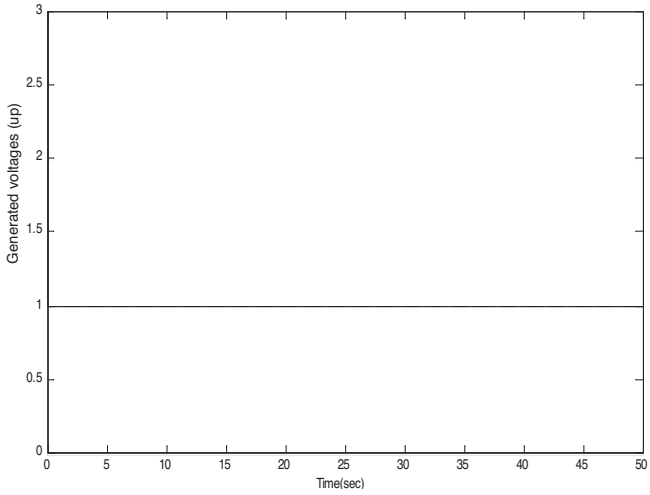

Figure 6.7: Generated voltages (Pu)

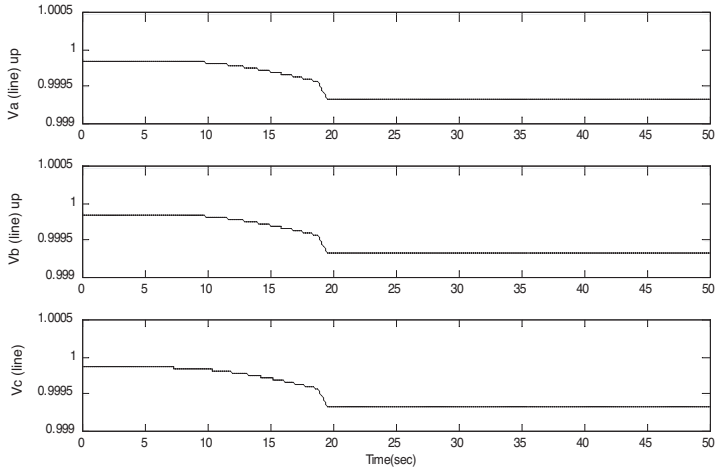

Figure 6.8: Grid terminals voltages (Pu)

4. CONCLUSION

A field oriented scheme is developed to control both rotor side current-source converter and line side current-source converter. Field orientation allows decoupled or independent control of both active and reactive power of DFIG. These techniques are based on the theory of controlling the d and q axes components of voltage or current in different reference frames. In this work, the stator flux oriented rotor current control, with decoupled control of active and reactive power is adopted. This scheme allows the independent control of the generated active and reactive power as well as the rotor speed to track the maximum wind power point. The controller used in vector controllers is of the PI type with varying proportional and integral gain.

REFERENCES

1. A. Rasmussens, BTM Consults (2005), International Wind Energy Development -World Market Update 2005, Forecast. Ringkøbing, Denmark, (2006) pp. 2006–2010.
2. Chowdhury Badrul H, Chellapilla Srinivas, "Double-fed induction generator control for variablespeed wind power generation" Electric Power Systems Research 76 (2006) , pp. 786–800
3. E. Muljadi, K. Pierce, P. Migliore, "Control strategy for variable speed stall regulated wind turbines", American Control Conference, vol. 3, 24–26 June, (1998), pp. 1710–1714.
4. E. Muljadi, C.P. Butterfield, "Pitch-controlled variable speed wind turbine Generation", IEEE Trans. Ind. Appl. 37 (1) (2001) pp. 240–246.
5. Hany M. Jabr, Narayan C. Kar, "Fuzzy Gain Tuner for Vector Control of Doubly-Fed Wind Driven Induction Generator", IEEE CCECE/CCGEI, Ottawa, 1-4244-0038-4(2006), pp.2266–2269.
6. R. Spee, S. Bhowmik and J. H. R. Enslin, "Novel control strategies for variable-speed doubly fed wind power generation systems," Renewable Energy, vol. 6 (1995), pp. 907–915.
7. R. S. Pena, J. C. Clare and G. M. Asher, "Doubly fed induction generator using back-to-back PWM converters and its application to variable-speed wind-energy generation", IEE Proc. Electric Power Applications, vol. 143, No. 3, (1996), pp. 231–341.
8. A. Tapia, G. Tapia, J.X. Ostolaza and J.R. Senz, "Modeling and control of a wind turbine driven doubly fed induction generator," IEEE Trans. on Energy Conversion, vol. 18(2003), pp.194–204.
9. Lie Xu , "Coordinated Control of DFIG's Rotor and Grid Side Converters During Network Unbalance" IEEE Trans. Power Electronics, vol. 23, No. 3, MAY (2008), pp.1041–1049.
10. Balasubramaniam Babypriya, Rajapalan Anita, "Modelling, Simulation and Analysis of Doubly Fed Induction Generator for Wind Turbines" Journal of Electrical Engineering, vol. 60, No. 2, (2009), pp.79–85.
11. Hopfensperger, B. Atkinson, D. Lakin, R. A, "Stator Flux Oriented Control of a Cascaded Doubly-Fed In- duction Machine", IEE Proc. Electr. Power Appl. 146 No. 6, (Nov1999), pp.597–605.
12. Koch, F. W. , Erlich, I. Shewarega, F. "Dynamic Simulation of Large Wind Farms Integrated in A Multi Machine Network", in Proceedings of 2003 IEEE PES General Meeting, Toronto, Canada, (July 13–17 2003).
13. MULLER, S. Deicke, M. De Doncker, R. W. "Doubly Fed Induction Generator Systems for Wind Turbines", IEEE Industry Applications Magazine 8 No. 3, (May/June 2002), pp. 26–33.

14. Chee-Mun. Ong", Dynamic Simulation Of Electronic Machinary using Matlab/Simulink", PRINTICE HALL, (1998).

15. Pete. Vas ", Vector Control Of AC Machines",Oxford University , UK.

16. P.C. Krause, O. Wasynzuk, S.D. Sudhoff, "Analysis of ElectricMachineryand Drive Systems", IEEE press, (2002).

17. P. Vas, "Vector Control of AC Machines", New York, Oxford Univ. Press,UK, (1990).

18. R. Pena, J.C. Clare, G.M. Asher, "Doubly fed induction generator using back-to-back PWM converters and its application to variable-speed wind-energy generation", IEEE Proc.-Electr. Power Appl., Vol. 143, No. 3, (May 1996).

19. Siegfried Heier, "Grid Integration of Wind Energy Conversion Systems", ISBN 0-471-97143- X, John Wiley & Sons Ltd, (1998).